J. Phys. Chem. Solids Vol. 51, No. 4, pp. 367–372, 1990
Printed in Great Britain.

0022-3697/90 \$3.00 + 0.00

DEFECT STRUCTURE AND ION TRANSPORT IN LaOBr

M. S. ISLAM†
Corporate Research Laboratories, Eastman Kodak Company, Rochester, NY 14650–2021, U.S.A.

(*Received* 10 *October* 1989; *accepted* 15 *November* 1989)

Abstract—A theoretical survey, based on atomistic computer simulation methods, of defect energetics in LaOBr is presented. Lattice potentials that include three-body terms have been developed, which correctly reproduce the layered tetragonal structure and are used in calculations of the formation energies of point defects and migration activation energies. The concentration of interstitial ions is predicted to be negligible, with vacancy disorder favored in the pure material. Ionic conductivity is most likely to arise from the diffusion of Br^- ion vacancies via an interplanar mechanism. The defect energies of self-trapped hole species have been calculated and used to estimate excitation energies. The results find the out-of-plane Br_2^- configuration to be the most favorable V_k center, with comparable stability to the O^- hole center.

Keywords: LaOBr, computer simulation, phosphor, point defect, ion transport, PbFCl structure, V_k center.

1. INTRODUCTION

LaOBr exhibits highly efficient luminescence under X-ray, UV, and cathode-ray excitation, upon doping with different rare-earth activators [1–6]. It is thus a material of increasing technological importance owing to its practical applications, in particular for X-ray intensifying screens.

The precise mechanism of the photostimulated luminescence is still not completely understood, but it is thought to be strongly dependent upon the energetics and mobility of various hole and electron states, which in turn are related to the atomic defects that may be intrinsic to the material. Many of the electronic species have been examined in the isostructural barium fluorohalide phosphors by spin-resonance and optical techniques. These studies of BaFCl, for example, have identified the electron states as F-centers consisting of a chloride or fluoride ion vacancy occupied by an electron [7, 8], whereas the various hole states that have been identified include the V_k center represented by a Cl_2^- species in the crystal [9, 10].

Like the barium fluorohalide compounds, LaOBr crystallizes in the PbFCl-type structure (space group *P4/nmm*), as shown in Fig. 1. The structure is tetragonal with layers normal to the *c*-axis, consisting of close-packed oxide ion planes separated by lanthanum ions and two adjacent bromide ion planes.

Despite the number of experiments on the luminescence and optical properties of LaOBr, no extensive study dealing with point defects or ion-transport mechanisms has been published. It is apparent that a complete characterization of the intrinsic defect structure is important in any attempts to optimize the luminescent properties of the material. The purpose of this study is to investigate theoretically the energetics of defect formation in undoped LaOBr. The atomistic simulation techniques developed in the HADES [11] and CASCADE [12] computer codes are employed, which have proved successful in elucidating the defect structure of other ionic and semi-ionic systems [13, 14]. The present work extends the recent theoretical studies of alkaline-earth fluorohalides [15, 16] and PbFCl [17] to include the structural modeling of LaOBr, a material thought to have an increased degree of covalent character. A number of atomic defects, such as vacancies or interstitials, and self-trapped hole species are considered, following closely this earlier work. In addition, we describe the calculation of activation energies associated with anion vacancy diffusion by a variety of migration mechanisms.

2. METHOD AND POTENTIALS

The simulation methods are based on a Born-model description of the polar solid with integral ionic charges. It is worth noting that the use of such a model does not necessarily imply that the electron-density distribution corresponds to a fully ionic description and that the general validity of the model is assessed primarily by its ability to reproduce observed crystal properties, a topic discussed in detail by Catlow and Stoneham [18]. The short-range interaction between closed-shell ions is represented by central force potentials of the form:

$$V(r) = A \exp(-r/\rho) - C/r^6, \qquad (1)$$

where r is the interionic separation and A, ρ, and C

---

†Present address: Department of Chemistry, University of Surrey, Guildford GU2 5XH, U.K.

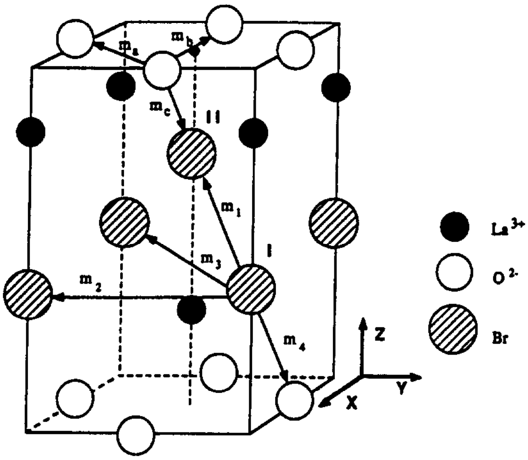

Fig. 1. Crystal structure of LaOBr, showing the possible mechanisms for anion vacancy migration.

are constants assigned to each ion–ion interaction. Ion polarization is treated by the shell model [19], which represents each ion in terms of a massless shell (of charge Y, simulating the valence shell electrons) and a core, coupled by a harmonic spring with force constant k. The free-ion polarizability α is then given by:

$$\alpha = Y^2/k. \tag{2}$$

The shell model has been shown to correctly simulate both dielectric and elastic properties, which is essential for reliable calculations of defect energies. The potential parameters for LaOBr were derived by a standard empirical fitting procedure to minimize the internal basis strains and bulk lattice strains acting on the structure, using the observed cell dimensions. It was found, however, that a satisfactory model for LaOBr must extend beyond two-body potentials. The bond-bending formalism was implemented, which has been applied successfully to the modeling of α-SiO_2 [20] and La_2CuO_4 [21]. This adds a three-body term to specified bond angles and has the form:

Table 2. Comparison of calculated and observed bond lengths (in Å)

Bond	r(expt)†	r(calc)	Δ
La–O	2.400	2.389	0.011
La–Br^I	3.301	3.306	0.005
La–Br^{II}	3.495	3.549	0.054
O–O	2.941	2.915	0.026
O–Br^I	3.407	3.451	0.044
Br^I–Br^{II}	3.554	3.528	0.026

† From Ref. 5.

$$E(\theta) = \tfrac{1}{2}k_B(\theta - \theta_0)^2, \tag{3}$$

where k_B is the bond-bending force constant and θ_0 the equilibrium bond angle. In the case of LaOBr, three-body terms were used for the triad Br^{II}–Br^I–O($\theta_0 = 95°$), where Br^I and Br^{II} represent two bromide ions in adjacent planes, as shown in Fig. 1. The resulting potential parameters used in the present study are reported in Table 1.

The tetragonal distortion is at the center of the difficulties in modeling this material. Employing only two-body potentials tended to produce large strains along the c-direction in the equilibrated structure. The effect of including the bond-bending potential is to reduce these strains, to yield an equilibrium structure that is close to the observed structure. Table 2 lists the calculated and experimental bond lengths, with the largest deviation of only ~0.05 Å for the La–Br^{II} bond. By explicitly including bond-bending terms we have attempted to account for any covalency effects in the material. Indeed, the decreasing role of purely electrostatic effects on going from LaOF to LaOI in the oxyhalide series has been previously suggested, based upon the observation that the coordination between La^{3+} and the halide ions varies considerably, whereas the La–O

Table 1. Interatomic potential parameters for LaOBr

(a) Short range Interaction	A(eV)	ρ(Å)	C(eVÅ^6)
La–La	24244.5	0.3446	0.0
La–O	1648.6	0.3590	52.6
La–Br	29882.7	0.2716	174.9
O–O	22764.3	0.1490	260.0
O–Br	6287.9	0.3269	139.6
Br–Br	4259.6	0.3749	196.3
(b) Shell model			
	Species	$Y(e)$	k(eVÅ^{-2})
	La^{3+}	−0.25	145.0
	O^{2-}	−2.389	42.0
	Br^-	−2.094	18.3
(c) Three-body			
	Central atom	k_B(eVrad^{-2})	θ_0
	Br^I	4.98	95

Table 3. Computed properties of the perfect crystal

Property	LaOBr
Lattice energy (eV)	−57.45
c/a	1.809 (1.777†)
Elastic constants (10^{11} dyn cm^{-2})	
c_{11}	21.45
c_{12}	4.31
c_{13}	3.30
c_{33}	18.14
c_{44}	4.25
c_{66}	7.31
Dielectric constants	
ϵ_0	22.82, 6.64
ϵ_∞	2.30, 2.23

† Observed value.

distance remains essentially the same (at about 2.40 Å) [22].

The elastic and dielectric constants for the perfect crystal have also been calculated and reported in Table 3. Unfortunately, corresponding experimental data for comparison are unavailable. Nonetheless, the absence of any negative values for the computed constants indicates that there are no instabilities in the potential model, although calculation of the phonon dispersion curves is necessary for a more rigorous test. After attaining the minimum energy configuration of the perfect lattice, defect energies are calculated using procedures based on the well-established Mott–Littleton method [23, 24]. This is basically a two-region strategy, whereby the crystal immediately surrounding the defect, containing typically 100–200 ions, is equilibrated atomistically, whereas the more distant regions of the crystal are treated as a continuum using the calculated dielectric constant. The explicit simulation of the inner region uses efficient energy-minimization methods based on a modified Newton–Raphson procedure [11, 12], which makes use of first and second derivatives of the energy function. Details of the simulation techniques used and their application to other solids are available elsewhere [13, 14].

3. RESULTS AND DISCUSSION

3.1. *Atomic defects*

The energies of isolated vacancies and interstitials for both anion and cation species have been calculated and are presented in Table 4. The calculations were performed with the atomistically simulated inner region containing 200 ions, which is large enough for full convergence. It is noted that identical inner regions are used in all the calculations, thus ensuring that any errors arising from the two-region strategy approximation will be largely self-cancelling quantities. The most stable interstitial position in the perfect crystal is found to lie in the face of the unit cell consisting of La^{3+} and Br^- ions, but between the two adjacent Br^- planes.

Table 4. Calculated formation energies of point defects†

Defect	E(eV)
Vacancies	
La	41.55
O	21.77
Br	2.14
Interstitials	
La	−19.60
O	−8.16
Br	9.29

† Energy is referenced to zero for defect species at infinity.

Table 5. Calculated formation energies of Frenkel and Schottky disorder

Defect	E(eV per defect)
Frenkel	
La	10.98
O	6.81
Br	5.72
Schottky	
LaOBr	2.67
La_2O_3	4.46
$LaBr_3$	1.08

The individual point defect energies are then combined to give estimates of formation energies for Frenkel- and Schottky-like disorder. The Frenkel energy is evaluated as the sum of vacancy and interstitial energies, and the Schottky energy is the sum of vacancy energies minus the appropriate cohesive energy. The resulting values are reported in Table 5 as the energy per constituent defect (for example, the Frenkel-pair energy divided by two).

Since the Frenkel energies are higher than the Schottky energies, interstitial formation is unlikely to be significant in LaOBr. The calculations also predict that the predominant mode of intrinsic disorder is of the Schottky type involving La^{3+} and Br^- vacancies. This could possibly lead to a degree of non-stoichiometry or antisite formation, with O^{2-} substituting for Br^-. In any case, vacancy disorder should dominate in the pure material. Most notably, vacancies are more easily formed on bromide ion sites than on the oxide ion sites. This conclusion is in line with the results of defect simulations for other PbFCl structured crystals [15–17], where it is found that the Schottky-like defect involving the larger halide ion is the most favored intrinsic disorder. Hence, the ion-transport properties of LaOBr will be dominated by the diffusion of vacancies rather than interstitials.

3.2. *Ion diffusion*

Since ion diffusion is controlled principally by the energy parameters associated with the formation and migration of point defects, activation energies for anion-vacancy migration were also examined. The various mechanisms considered are illustrated in Fig. 1 and involve oxygen-vacancy migration (labeled m_a, m_b, m_c) and bromide-vacancy migration (labeled m_1–m_4). These mechanisms were originally enumerated for this structure by Halff and Schoonman from

Table 6. Calculated activation energies for anion-vacancy migration

Mechanism	E(eV)
O vacancy	
m_a	0.44
m_b	2.64
m_c	NC†
Br vacancy	
m_1	0.39
m_2	2.60
m_3	9.39
m_4	NC†

† Non-convergence of calculation due to excessive core displacement.

an ionic-conductivity study of PbFCl [25]. Ion transport within the *ab* plane can be effected by mechanisms m_a, m_b, m_2, and m_3, whereas the other mechanisms, m_c, m_1, and m_4, have components both parallel and perpendicular to the c-axis. Note that although conductivity studies provide accurate activation energies, it is not always possible to associate the observed values with a particular diffusion mechanism. Defect calculations can be used to resolve this difficulty.

The energy barriers to migration are evaluated by calculating the defect energy of the migrating ion as a function of position along the diffusion path. In every case, the saddle-point configuration, from which the activation energy is derived, was found to be midway between the two anion sites involved in the mechanism.

Examination of the calculated activation energies reported in Table 6 reveals that the lowest energy barrier is associated with bromide-vacancy migration via the interplanar mechanism m_1. This diffusion mechanism is thus favored over intraplanar migration or migration to the oxygen site. A similar result was found for chloride-vacancy migration in PbFCl [17, 25]. However, the calculated values also show that the intraplanar O^{2-} vacancy mechanism m_a has an almost identical energy barrier. Solely on the basis of activation energies, vacancy migration via mechanisms m_a and m_1 would be expected to dominate the ion-transport properties. However, the migration of vacancies of a particular type is also controlled by formation energetics. In view of the result showing Schottky-like disorder involving Br^- vacancies as the most favorable intrinsic defect, making the concentration of thermally generated O^{2-} vacancies negligible compared with that of Br^- vacancies, diffusion associated with mechanism m_1 will predominate in the pure crystal. Oxide vacancy conduction will only become important when LaOBr contains a high concentration of impurities, owing to the high formation energy of the corresponding Schottky defect.

As might be expected from arguments based on geometry and steric factors, the intraplanar mechanisms m_b and m_3 seem unlikely to be of any significance. This view is confirmed from the calculations which find their energy barriers highly prohibitive. We have attempted to calculate the activation energies for mechanisms m_c and m_4 that relate to antisite disorder, in which a bromide ion migrates into an oxide vacancy and an oxide ion migrates into a bromide vacancy. The potentials for LaOBr were found to be unstable to this type of diffusion, leading to non-convergence of the defect simulations. The activation energy for La^{3+} vacancy migration was also calculated and found to be in excess of 20 eV, thus proving to be unimportant in LaOBr.

The Br^- vacancies are predicted to be the most mobile species and shown to diffuse through the bulk by an interplanar mechanism involving zig-zag-type motion between two adjacent Br^- planes. We, therefore, expect anisotropic ionic conductivity to be exhibited in the LaOBr crystal, although at present there are no corresponding quantitative conductivity data. Nevertheless, there are some mobility data for LaOF [26], which show an activation energy in the range 0.6–0.8 eV. It is apparent that the diffusion rate in LaOBr is faster than that exhibited in LaOF. This result is not unexpected when considering the more marked layered nature of the oxybromide in comparison with the oxyfluoride.

3.3. *Hole centers*

The relative stability of self-trapped hole species, including V_k and O^- centers, is now considered. These hole centers may be important in connection with the luminescent properties of LaOBr and the phosphor mechanism in particular. The V_k center is treated in terms of the "molecule in the crystal" model [27, 28], which assumes that the electronic properties of the center are those of an embedded X_2^- molecular ion, with the crystal environment only slightly perturbing its interatomic spacing. The hole is thus shared between two adjacent anions, with both ions moving off their normal lattice positions. The stabilization energy arises primarily from the binding energy of the molecule. The V_k center is typical of a wide range of binary halides and has also been detected in more complex systems, such as alkaline-earth fluorohalides [9, 10]. We should note that extensive theoretical studies of V_k centers have successfully applied the molecular anion model to these compounds [15, 27, 29, 30]. Such studies have also confirmed that two-site self-trapping is energetically more favorable than trapping on a single halide ion site or complete delocalization.

For the hole trapped on the oxygen sublattice, a small polaron model is assumed, in which the hole is localized on an oxide ion, giving an ionic species corresponding to O^- and self-trapped by its own polarization field. For this hole center, the same short-range potential is retained for the different charge-state.

In the present study, two V_k-center configurations for the Br_2^- were considered: a nearest-neighbor pair in the same plane (referred to as the in-plane Br_2^-)

Table 7. Hole center energies†

Defect	E_D(eV)	E_F(eV)‡
Br_2^- (in-plane)	4.74	8.12
Br_2^- (out-of-plane)	3.92	7.30
O^-	16.00	7.25

† Definitions of E_D and E_F in the text.
‡ Electron affinities used to calculate E_F are from Ref. 31.

and a pair in which the two component ions are in adjacent planes (referred to as the out-of-plane Br_2^-). In our treatment of V_k centers the relevant potentials for the Br_2^- molecular anion were taken from a study of caesium halides [29].

The defect energies, E_D, for the hole states are listed in Table 7. The V_k energies correspond to the energy required to remove two lattice Br^- ions separately to infinity and then replace them with a Br_2^- defect molecule (originally with the component ions separated); likewise, the defect energy for O^- involves the removal of a lattice O^{2-} ion to infinity, its ionization to O^-, and subsequent return to the lattice. In both cases, the surrounding crystal lattice is allowed to relax to equilibrium. Alternatively, for the large polaron there is no contribution from lattice distortion, but it is stabilized by an energy equal to approximately half the rigid bandwidth. In view of the fact that experimental data for the bandwidths are not available specifically for LaOBr, we were unable to compare the stability of the large polaron relative to the small polaron. By combining the calculated energies for the isolated hole centers, E_D, with appropriate electron affinities of the free ions [31], it is possible to estimate excitation energies or hole formation energies E_F, with respect to electrons in the vacuum. For O^- this energy corresponds essentially to photoionization from the oxygen $2p$ band.

Examination of the resulting values, given in Table 7, reveals two main features. First, the out-of-plane Br_2^- configuration is predicted to be the most favorable V_k center. Although there are no corresponding experimental data for LaOBr, it is interesting to note that only the out-of-plane X_2^- V_k center has been observed in the BaFX crystals (where X = Cl or Br) [9, 10], which would be consistent with our results. Second, the calculations show that the formation energetics for the out-of-plane Br_2^- and O^- hole centers are very similar. It is therefore difficult to distinguish the intrinsic defect that would predominate following, for example, X-irradiation. We note that there are uncertainties in the exact magnitude of the hole-formation energies due to uncertainties in the free-ion terms that must be added to the calculated defect-energy terms. Moreover, an additional problem arises from the uncertain role of the electron carrier formed during the photoionization process. The electron may be trapped at an anion vacancy, forming an F-center, or at a dopant ion. In any case, the energy level of the electron trap with respect to the vacuum would be required for comparison of relative stabilities. Clearly, spin-resonance experiments would be useful to discern the most stable hole configuration.

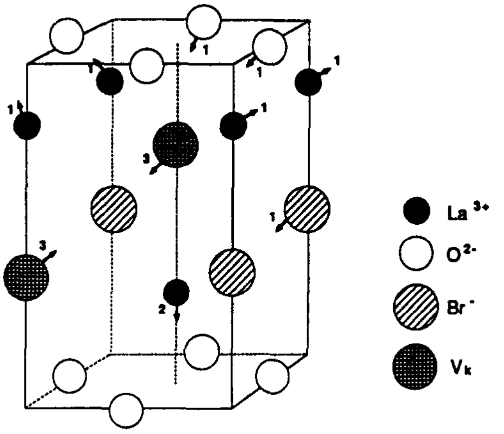

Fig. 2. Relaxation of lattice ions associated with the formation of the out-of-plane Br_2^- V_k center. The major displacements are indicated in 10^{-1} Å.

The simulation codes employed also provide detailed information on the relaxed positions of ions about the defect species. The calculations for the O^- center found no significant movement of ions. In contrast, the formation of the V_k center yields substantial relaxations of the component ions and the surrounding host lattice ions. The resulting ion movements for the most stable V_k center are shown in Fig. 2. In Table 8, the interatomic spacings within the Br_2^- defect molecules following relaxation are listed, together with the bond distances for the free molecular anions and the perfect crystal for comparison.

Examination of Fig. 2 reveals large displacements associated with the V_k-center ions moving towards one another, causing the $(Br–Br)^-$ spacing to decrease by ~20% from the perfect crystal value. This bond length contraction is as expected in view of the fact that, when a hole is trapped to form the V_k center, an antibonding electron is lost. We also find the neighboring La^{3+} ions moving away from the Br_2^- molecular anion by as much as 0.2 Å and a small displacement of two O^{2-} ions towards the defect. The out-of-plane V_k center thus induces a slight distortion

Table 8. V_k-center interatomic separations (in Å)

Configuration	$R(V_k)$	R(free X_2^-)†	R(crystal)
Br_2^- (in-plane)	3.37	2.90	4.159
Br_2^- (out-of-plane)	2.87	2.90	3.554

† From Ref. 32.

in the local structure. Finally, the entries in Table 8 indicate only a small difference between the out-of-plane Br_2^- interatomic spacing and the free-molecule bond length of 2.90 Å. This result is consistent with the proposed model for the V_k center, as an X_2^- molecular anion embedded in a distorted host crystal, with only a small deviation in the molecular geometry. The molecular-anion model can be tested further by comparing predicted optical transition energies and EPR parameters with observed V_k center parameters, when such data become available.

4. CONCLUSION

Interatomic potentials have been derived for LaOBr that correctly reproduce the low-symmetry structure, after incorporating three-body terms. The subsequent series of defect simulations have established a good basis for developing an understanding of the defect chemistry of the pure material. First, the Schottky-like defect consisting of La^{3+} and Br^- vacancies is shown to be the predominant intrinsic disorder, with a negligible concentration of interstitials. Second, the diffusion calculations predict that ionic conductivity will be associated with interplanar Br^- vacancy migration. On account of this type of motion and the layered nature of the crystal structure, anisotropic ion transport properties are anticipated. Finally, the out-of-plane Br_2^- is shown to be the most favorable V_k center, although the excitation energetics are very similar to those for the O^- hole species. The relative stability of forming V_k and O^- centers is difficult to distinguish owing to the unknown role of the electron carrier formed during photoionization. Despite this problem, the calculations suggest that these trapped-hole centers may be important intermediates in the luminescence process.

As remarked earlier, there are at present limited experimental data with which comparisons may be made and, thus, the results of our calculations have a clear predictive value. Indeed, one of the aims of the present study is to encourage further experimental work in this area towards testing these predictions.

Acknowledgements—I am grateful to Roger Baetzold for many helpful discussions on this work.

REFERENCES

1. Blasse G. and Bril A., *J. chem. Phys.* **47,** 1920 (1967).
2. Holsa J., Leskela M. and Niinisto L., *J. Solid St. Chem.* **37,** 267 (1981).
3. De Maayer P. and Bollen R., *J. electrochem. Soc.* **130,** 437 (1983).
4. Mo L. Y., Guillen F., Fouassier C. and Hagenmuller P., *J. electrochem. Soc.* **132,** 717 (1985).
5. Haeuseler H. and Jung M., *Mater. Res. Bull.* **21,** 1291 (1986).
6. Blasse G., Sytsma J. and Brixner L. H., *Chem. Phys. Lett.* **155,** 64 (1989).
7. Nicklaus E. and Fisher F., *Phys. Status Solidi (b)* **52,** 453 (1972).
8. Niklas J. R., Herder G., Yuste M. and Spaeth J.-M., *Solid St. Commun.* **26,** 169 (1978).
9. Yuste M., Taurel L. and Rahmani M., *Solid St. Commun.* **17,** 1435 (1975).
10. Eachus R. S. and Nuttall R. H. D., *Abstract* TU-P58, *International Conference on Defects in Insulating Crystals*, Parma, Italy (1988).
11. Norgett M. J., AERE Report No. R7650 (unpublished) (1974).
12. Leslie M., *Solid. St. Ionics* **8,** 243 (1983).
13. Catlow C. R. A. and Mackrodt W. C., *Computer Simulation of Solids, Lecture Notes in Physics*, No. 166. Springer, Berlin (1982).
14. Agullo-Lopez F., Catlow C. R. A. and Townsend P. D., *Point Defects in Materials*, Chap. 11. Academic Press, London (1988).
15. Baetzold R. C., *Phys. Rev.* **B36,** 9182 (1987).
16. Baetzold R. C., *J. Phys. Chem. Solids* **50,** 915 (1989).
17. Islam M. S., *J. Solid St. Chem* (in press).
18. Catlow C. R. A. and Stoneham A. M., *J. Phys. C* **16,** 4321 (1983).
19. Dick B. G. and Overhauser A. W., *Phys. Rev.* **112,** 90 (1958).
20. Sanders M. J., Leslie M. and Catlow C. R. A., *J. Chem. Soc. Chem. Comm.*, 1271 (1984).
21. Islam M. S., Leslie M., Tomlinson S. M. and Catlow C. R. A., *J. Phys. C* **21,** L109 (1988).
22. Holsa J. and Porcher P., *J. chem. Phys.* **76,** 2790 (1982).
23. Mott N. F. and Littleton M. J., *Trans. Faraday Soc.* **34,** 485 (1938).
24. Lidiard A. B., *J. chem. Soc. Faraday Trans.* 2, **85,** 341 (1989).
25. Halff A. F. and Schoonman J., *J. Solid St. Chem.* **27,** 397 (1979).
26. Brice J. F., *Ann. Chim. Fr.* **7,** 635 (1982).
27. Stoneham A. M., *Theory of Defects in Solids*. Clarendon Press, Oxford (1975).
28. Tasker P. W. and Stoneham A. M., *J. Phys. Chem. Solids* **38,** 1185 (1977).
29. Monnier R., Song K. S. and Stoneham A. M., *J.Phys. C* **10,** 4441 (1977).
30. Cade P. E., Stoneham A. M. and Tasker P. W., *Phys. Rev.* **B30,** 4621 (1984).
31. Dasent W. E., *Inorganic Energetics*. Penguin, London (1970).
32. Tasker P. W., Balint-Kurti G. G. and Dixon R. N., *Molec. Phys.* **32,** 1651 (1976).